Ab Initio Analysis of Electron Transport in Oligoglycines

ARTICLE *in* THE JOURNAL OF PHYSICAL CHEMISTRY C · SEPTEMBER 2007

Impact Factor: 4.77 · DOI: 10.1021/jp0749930

3 AUTHORS, INCLUDING:

Liuming Yan
Shanghai University
66 PUBLICATIONS **832** CITATIONS
SEE PROFILE

Jorge Seminario
Texas A&M University
232 PUBLICATIONS **4,949** CITATIONS
SEE PROFILE

Ab Initio Analysis of Electron Transport in Oligoglycines

Eddy J. Bautista,[†] Liuming Yan,[†] and Jorge M. Seminario*[,†,‡]

Department of Chemical Engineering, and Department of Electrical and Computer Engineering, Texas A&M University, College Station, Texas

Received: June 26, 2007; In Final Form: July 27, 2007

We study the electrical characteristics of a group of glycine oligopeptides (1-, 3-, 6-, and 9-mers) molecules attached to gold nanoelectrodes using a combined density functional theory—Green's function approach. Our procedure considers the applied voltage through the molecule and contacts, recalculates self-consistently the molecular orbitals, Hamiltonian and overlap matrices at each applied voltage, and uses these results to estimate the current−voltage characteristics such that the chemistry of the molecule is fully considered when including the effect of the nanoelectrodes. Our results show that oligoglycines can be used to tailor specific properties for the fabrication of molecular devices and the characteristics may be strongly affected by the few contact atoms addressing the molecule. Oligoglycines show transport behaviors that go from ohmic conductance to Schottky barriers as the length of the oligomers and conformation of the electrode atoms vary.

1. Introduction

Despite the great progress in the experimental measurement of electron transport in molecular junctions, it is still a great challenge to understand the current−voltage ($I-V$) characteristics of a single molecular junction. In 1997, Reed et al.[1] measured the $I-V$ of benzene-1,4-dithiol molecular junction fabricated by the mechanically controllable break junction technique with the molecule self-assembled between two facing gold electrodes. After this measurement, much more effort has been conducted in this field. Mantooth and Weiss[2] revised several of the experimental methods to assemble molecules between electrodes for the measurement of molecular $I-V$ characteristics. For a comparative review of measurements and calculations of low-bias, room-temperature $I-V$ measurements of alkane chains and conjugated molecules, the reader is referred to refs 3−7. Certainly, electron transport in single-molecule junctions has also attracted great theoretical interests. Most calculations are mainly based on quantum transport theory by combining the Green's function techniques and quantum mechanics at different levels of theory. For example, Basch and Ratner[8] applied density functional theory to an atomistic model composed of a four-atom gold cluster and a thiol molecule and found that the sulfur atom favors a twofold bridge site.

One of the great challenges to experimental measurement and theoretical calculations of $I-V$ characteristics is reproducibility. Established from our experiences of the macroscopic world, reproducibility has become one of the criteria to judge if experiments are successful or not. However, this matching experiment−theory may represent an unreachable target and be simply limited to complementary information because single molecular junctions could never be reproducible as reproducibility is only applicable to the macroscopic world because of statistical averages over a large number of samples. However, the construction of single molecular junctions goes even further beyond this statistical problem. If we want to have reproducible results, we are demanding that a macroscopic number of molecules be used to construct a junction and ∼20−30 molecules should always be positioned exactly in the same region of 1−2 nm^2. By any means, this is the most challenging and perhaps unreachable goal, no matter what technology is used.[9]

A feature that most of the calculations have in common so far is the attachment of the molecular devices to microscopic contacts or electrodes. Although this approach matches with the experiments being performed if a lucky and very remote coincidence allows us to have the same experimental and theoretical structures, it is totally incompatible with the technology for which this device could be used. Molecular devices have to be connected to nanometer-sized contacts, not to microscopic ones. As in standard electronics, the transistors in an integrated circuit are connected to contacts ∼20 nm wide; molecules in a molecular electronics technology should be connected to contacts even smaller. Otherwise, for instance using contacts of 1 mm, a today's 1 cm^2 Pentium chip would be of the size of a football stadium. For review work of possible scenarios the readers are forwarded to refs 10−16.

Recently, we have calculated $I-V$ characteristics of benzenedithiol,[17] thiotolane,[18] oligo(nitro-ethynylphenyl)thiol,[19] thioalkane and polyynes,[20,21] cobalt complexes,[22] and oligoanilines.[23] In these calculations, we combined density functional theory with the Green's function theory and developed a first-principle method to calculate the $I-V$ characteristics of molecules assembled between two electrodes.[17,23] We also found that negative differential resistance (NDR), an important feature for building two terminal logical molecular devices, is ubiquitously achievable in nanoscaled interfaces.[24,25]

Oligoglycine is the simplest oligopeptide. It has applications in medicine due to its compatibility with living cells.[26] Oligoglycine could form fibrous microtubes.[26] One of the potential applications of fibrous oligoglycine is to transmit signals between molecular devices.[27,28] In this work, we analyze the effects of the geometry of nanosized contacts on the $I-V$ characteristics of a group of oligoglycine molecular junctions, $[Au_{bulk}Au_x]-[S-Gly_n-S]-[Au_xAu_{bulk}]$, where Gly_n, $n = 1$, 3, 6, and 9, represents a monomer, trimer, hexamer, or nonamer,

[†] Department of Chemical Engineering.
[‡] Department of Electrical and Computer Engineering.

10.1021/jp0749930 CCC: $37.00
Published on Web 09/12/2007

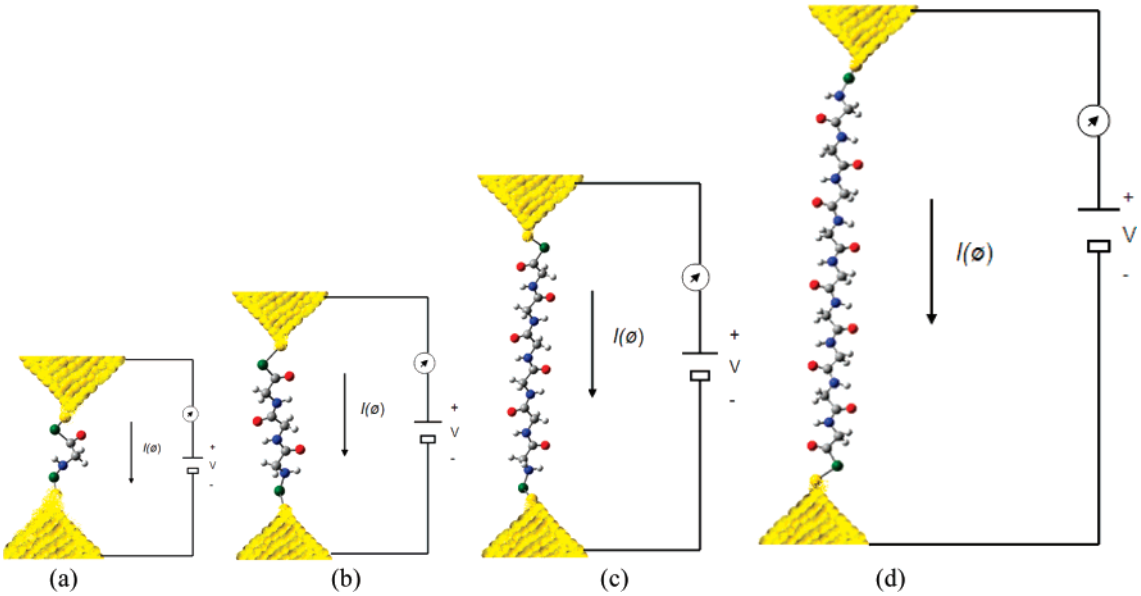

Figure 1. Molecular junctions for the glycine monomer (a), trimer (b), hexamer (c), and nonamer (d), $[Au_{bulk}Au_x]-[S-Gly_3-S]-[Au_xAu_{bulk}]$, attached to the continuum through one, two, or three gold atoms. Current, *I*, through the molecule is calculated considering the effect of the electric field at each applied voltage *V* (or Ø) on the electronic structure of the molecule using the B3PW91/LANL2DZ/6-31G* level of theory and the Green functions formalism to include the effect of the continuum calculated using periodic boundary conditions at the B3PW91/LANL2DZ level of theory. Au (yellow), S (green), N (blue), O (red), C (dark gray), H (clear gray).

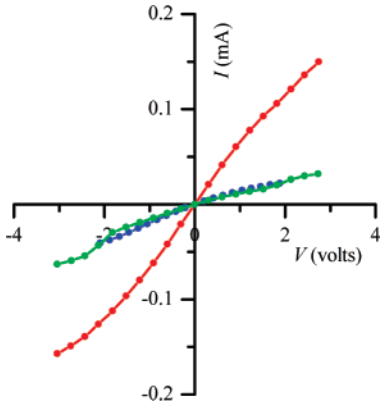

Figure 2. *I*−*V* characteristics of the glycine molecular junctions $[Au_{bulk}Au_x]-[S-Gly-S]-[Au_xAu_{bulk}]$, $x = 1$ (blue), $x = 2$ (red), and $x = 3$ (green).

respectively, of oligoglycine. $[Au_{bulk}Au_x]-$ and $-[Au_xAu_{bulk}]$ represent the left and right, respectively, gold nanoelectrode attached to the glycine through *x* gold atoms. The nanoelectrodes could have one, two, or three gold contact atoms ($x = 1$, 2, or 3) attaching the molecule as depicted in Figure 1, and their geometries are different than those from isolated gold clusters.[29] The calculations are based on a formalism that combines density functional theory and Green's function implemented in our program GENIP.[17,19,21,23,30,31]

2. Methodology

The electronic structure calculations are performed using density functional theory as coded in the GAUSSIAN 03 program[32] using the B3PW91 hybrid functional, a combination of the Becke3 (B3)[33] exchange functional and the Perdew−Wang (PW91)[34,35] correlation functional. The quasi-relativistic pseudopotential and basis set LANL2DZ[36] is used for Au, and the basis set 6-31G*[37] is used for C, H, O, N, and S. All molecules are optimized to minimize their total energies using the Berny algorithm,[38] which calculates the derivatives of the total energy with respect to the Cartesian coordinates of all atoms. In order to ensure that all the atomistic systems are optimized to local minimum, optimizations are followed by a second-derivative calculation to obtain the Hessian matrix. If negative eigenvalues exist in the Hessian matrix, the structure is modified and reoptimized. Negative eigenvalues in the Hessian matrix relate to saddle points or unstable geometrical conformations. The convergence thresholds for self-consistency of the auxiliary noninteracting electronic wave function are set, respectively, to 10^{-6} and 10^{-8} for the root-mean-square density matrix difference and for maximum density matrix difference between consecutive iterations. These settings provide, within the level of theory, with correct energies for at least five decimal digits, with bond lengths for three digits, and with bond angles for one digit.

After the optimization of the molecular junctions, their Hamiltonian and overlap matrices with external field applied are evaluated using the GAUSSIAN program. By applying these results to our Green's function formalism, the electron transport characteristics including the density of states, the electron transport function, and *I*−*V* characteristics are calculated.

To obtain the current through the molecule, the Fermi level of the junction has been approximated to the center of the HOMO−LUMO gap; this seems to a good approximation widely used also by most of other groups. In the special case of gold, this HOMO−LUMO gap midpoint seems to converge nicely toward the experimental value of −5.31 eV as the number of gold atoms increases. However, even with a small number of gold atoms, the HOMO−LUMO midpoint lies very close to the experimental value of gold as can be seen in the results reported in the next section.

Recent details of the formalism in the program GENIP are described elsewhere,[23] and details of its development can be found in refs 17, 19, 21, and 31.

3. Results and Discussion

In order to study the influence of nanoelectrodes on the *I*−*V* characteristics of molecular junctions, 12 types of molecular junctions are studied. The molecular junctions, $[Au_{bulk}Au_x]-$

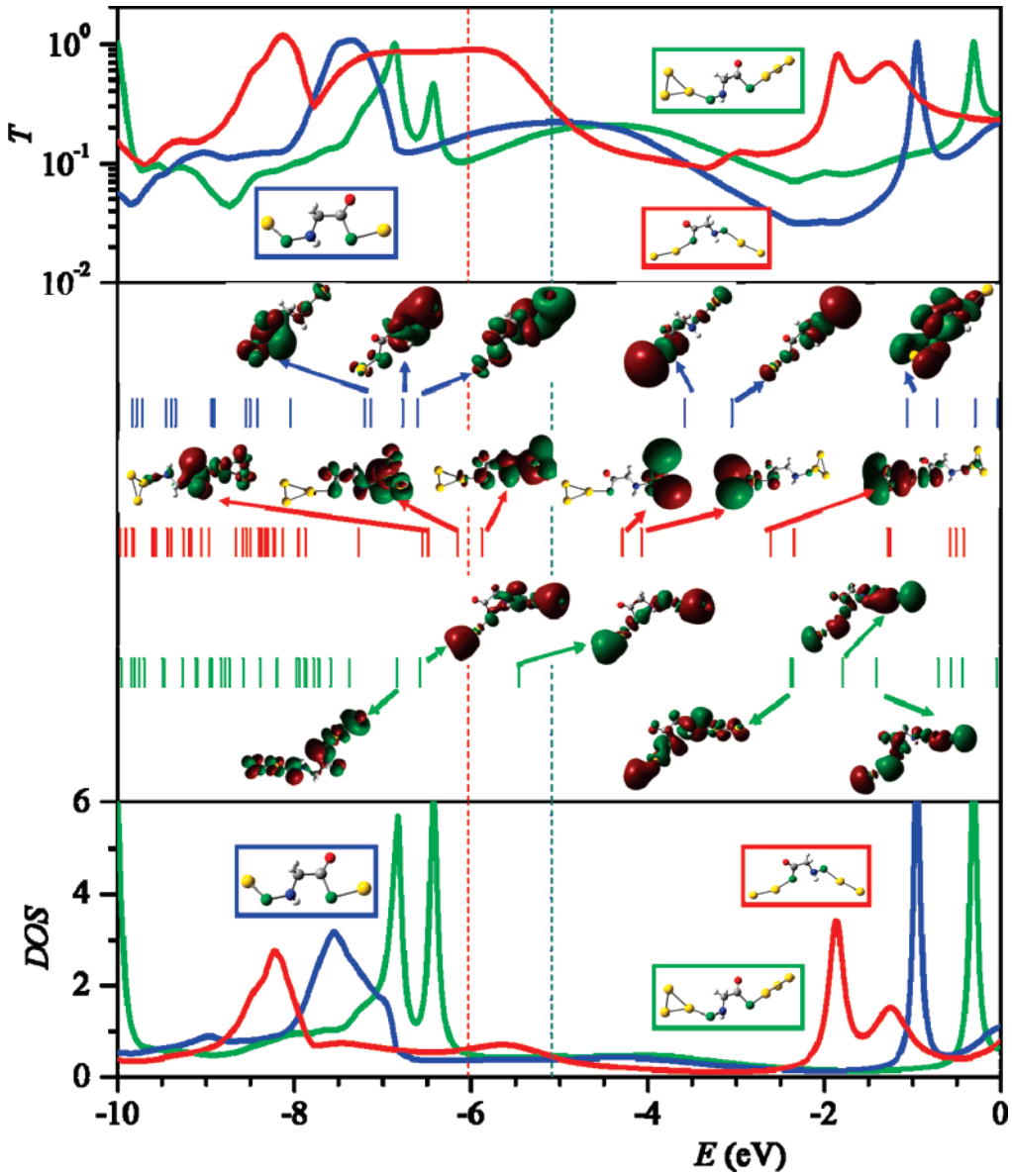

Figure 3. Electron transport characteristics of the [$Au_{bulk}Au_x$]−[S−Gly−S]−[Au_xAu_{bulk}] molecular junctions: (top panel) electron transmission function; (middle panel) molecular orbitals and their corresponding orbital energies in the vicinity of the Fermi level; (bottom panel) DOS. The vertical dashed lines represent the Fermi level (taken as the middle point of the HOMO−LUMO gap of the extended molecules). The nature of electrodes is determined by the number of gold atoms directly contacting the molecule; curves are color coded: blue for $x = 1$, red for $x = 2$, and green for $x = 3$. All calculations are carried out at the B3PW91/LANL2DZ/6-31G* theory level of theory.

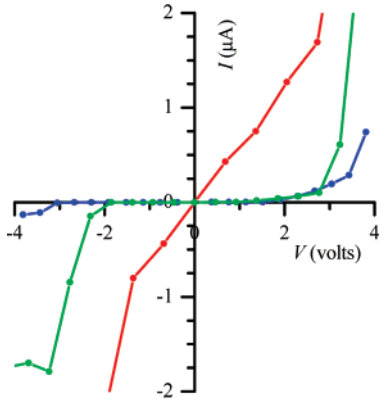

Figure 4. $I-V$ characteristics of the glycine molecular junctions [$Au_{bulk}Au_x$]−[S−Gly_3−S]−[Au_xAu_{bulk}], $x = 1$ (blue), $x = 2$ (red), and $x = 3$ (green).

[S−Gly_n−S]−[Au_xAu_{bulk}], are composed of three types of nanoelectrodes with $x = 1$, 2, or 3, and four types of molecules with $n = 1$, 3, 6, and 9 representing the glycine monomer, trimer, hexamer, and nonamer. The purpose is to evaluate the influence of the nanoelectrode on the characteristics of the molecular junctions.

Monomer. Figure 2 shows the $I-V$ characteristics of glycine monomer junctions ($n = 1$). The nanoelectrodes composed of one or three gold atoms have similar $I-V$ characteristics, whereas the one composed of two gold atoms has much higher conductance.

A single gold atom has only one valence electron. When the molecule attaches to the nanoelectrode with one gold atom, the sulfur atom bonded to gold, and there are no unpaired electrons left. However, when a second gold atom is added to each of the nanoelectrodes, there is an unpaired electron on at each end of the molecular junction. The unpaired electron is more suitable than the paired electrons to transport to the other nanoelectrode through the molecule; therefore, the nanoelectrode composed of two gold atoms enhances electron transport.

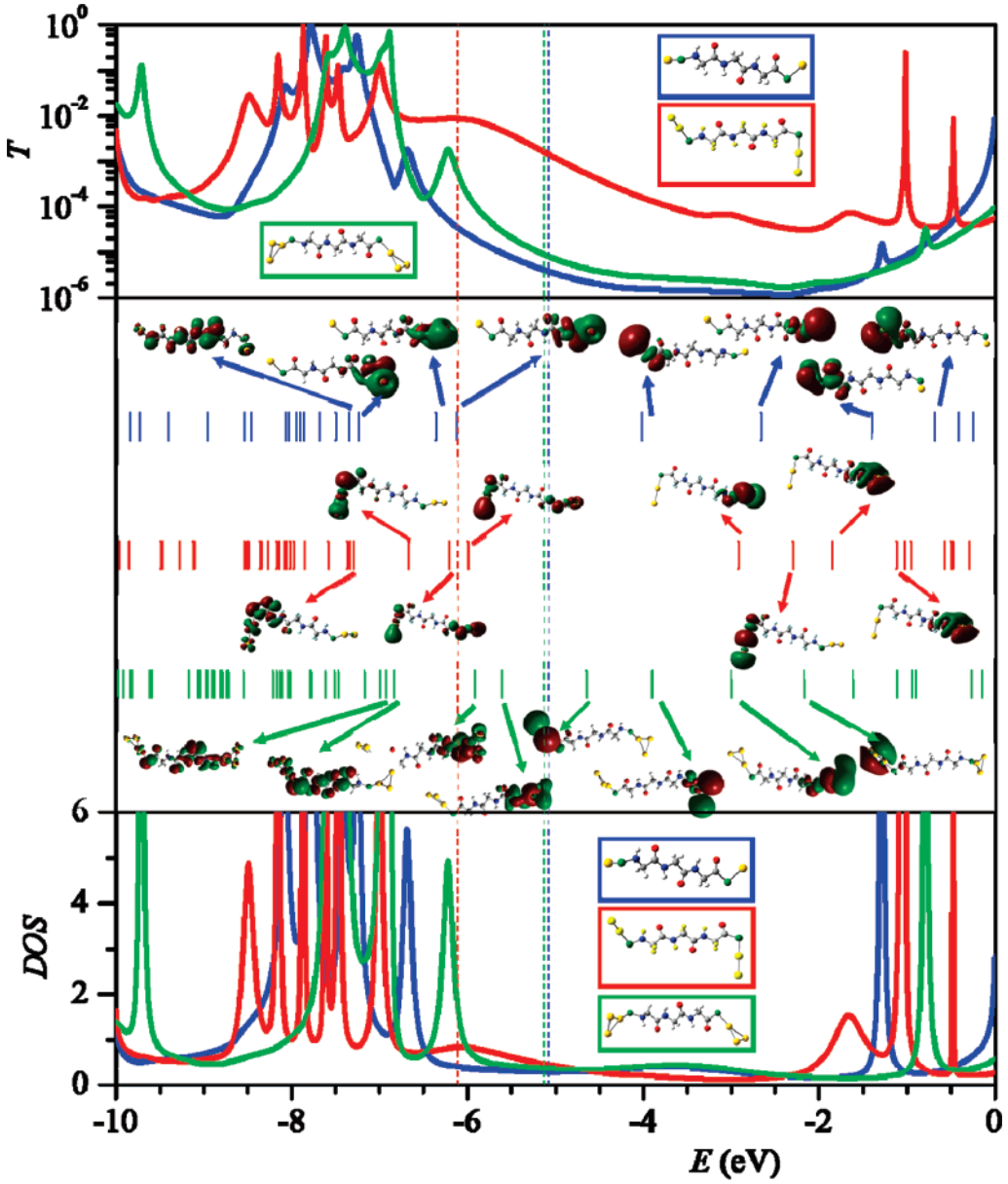

Figure 5. Electron transport characteristics of the $[Au_{bulk}Au_x]-[S-Gly_3-S]-[Au_xAu_{bulk}]$ molecular junctions: (top panel) electron transmission function; (middle panel) molecular orbitals and their corresponding orbital energies in the vicinity of the Fermi level; (bottom panel) DOS. The vertical dashed lines represent the Fermi level (taken as the middle point of the HOMO−LUMO gap of the extended molecules). The nature of electrodes is determined by the number of gold atoms directly contacting the molecule; curves are color coded: blue for $x = 1$, red for $x = 2$, and green for $x = 3$. All calculations are carried out at the B3PW91/LANL2DZ/6-31G* theory level of theory.

When a third gold atom is added to each of the nanoelectrodes, the electrons on the nanoelectrodes are paired. Thus, the molecular junction with nanoelectrodes composed of three gold atoms at each end exhibits similar $I-V$ characteristics as the one with only one gold atom.

In order to have a good understanding of the mechanism of $I-V$ characteristics of the glycine monomer molecular junctions, we study their density of states (DOS), molecular orbitals, and transmission functions.

From the middle panel of Figure 3 of the frontier molecular orbitals and orbital energies in the vicinity of the molecular junctions, it could be seen that the molecular junctions with nanoelectrodes with one or three gold atoms have similar Fermi energies, corresponding to the center of the HOMO−LUMO gap, whereas the Fermi energy for molecular junction with the nanoelectrode with two gold atoms is almost 1.0 eV lower.

Since there is an unpaired electron on each of the nanoelectrodes composed of two gold atoms, the 6s orbital of gold forms

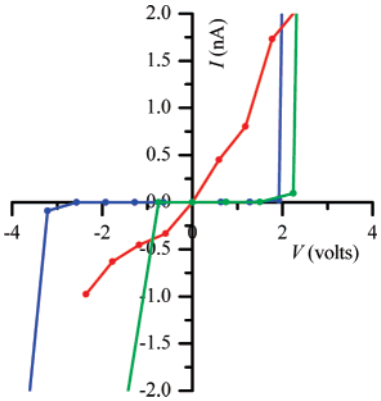

Figure 6. $I-V$ characteristics of the glycine molecular junctions $[Au_{bulk}Au_x]-[S-Gly_6-S]-[Au_xAu_{bulk}]$, $x = 1$ (blue), $x = 2$ (red), and $x = 3$ (green).

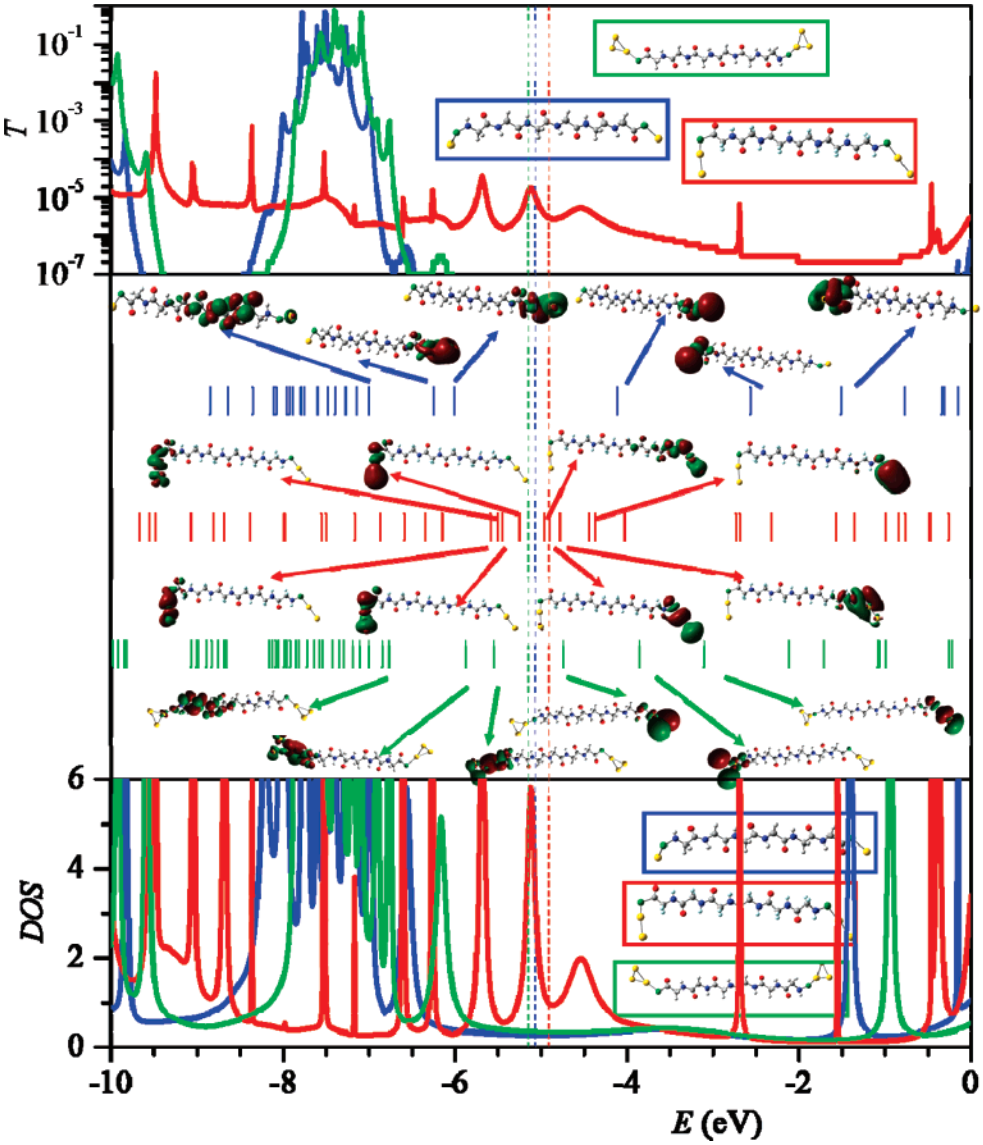

Figure 7. Electron transport characteristics of the $[Au_{bulk}Au_x]-[S-Gly_6-S]-[Au_xAu_{bulk}]$ molecular junctions: (top panel) electron transmission function; (middle panel) molecular orbitals and their corresponding orbital energies in the vicinity of the Fermi level; (bottom panel) DOS. The vertical dashed lines represent the Fermi level (taken as the middle point of the HOMO−LUMO gap of the extended molecules). The nature of electrodes is determined by the number of gold atoms directly contacting the molecule; curves are color coded: blue for $x = 1$, red for $x = 2$, and green for $x = 3$. All calculations are carried out at the B3PW91/LANL2DZ/6-31G* theory level of theory.

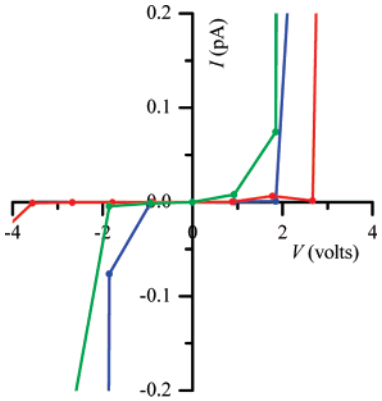

Figure 8. $I-V$ characteristics of the glycine molecular junctions $[Au_{bulk}Au_x]-[S-Gly_9-S]-[Au_xAu_{bulk}]$, $x = 1$ (blue), $x = 2$ (red), and $x = 3$ (green).

the HOMO and LUMO of the molecular junction, and the unpaired electrons on each side filled into the HOMO (Figure 3). Since these unpaired electrons are physically separated, the repulsion energy is lower than that of the paired electrons on the same nanoelectrode. Thus, the HOMO and LUMO energies of the molecular junctions with the nanoelectrode composed of two gold atoms are lower than that composed of one or three gold atoms.

Trimer. The DOS of the three glycine trimers in between the gold junctions show systematic changes from $x = 1$ to 3 (Figure 3). For the molecular junction with $x = 3$, there are two peaks below the Fermi level locating at about −6.5 and −7.0 eV, respectively. As the number of contact atoms decreases, the peak height decreases, the peak width increase, and the peak position goes to a lower energy; as a result, the two peaks combined into a flat peak for molecular junction with $x = 2$ and 3.

In the case of the molecular junction with $x = 1$, the peak has a shoulder at its right, whereas for the molecular junction with $x = 2$, the peak shoulder is at its left side. The changing trends of the peaks above the Fermi level are similar to the ones below the Fermi level. The peaks are shifted to a lower energy as the number of contact atoms decreases in the nanoelectrode.

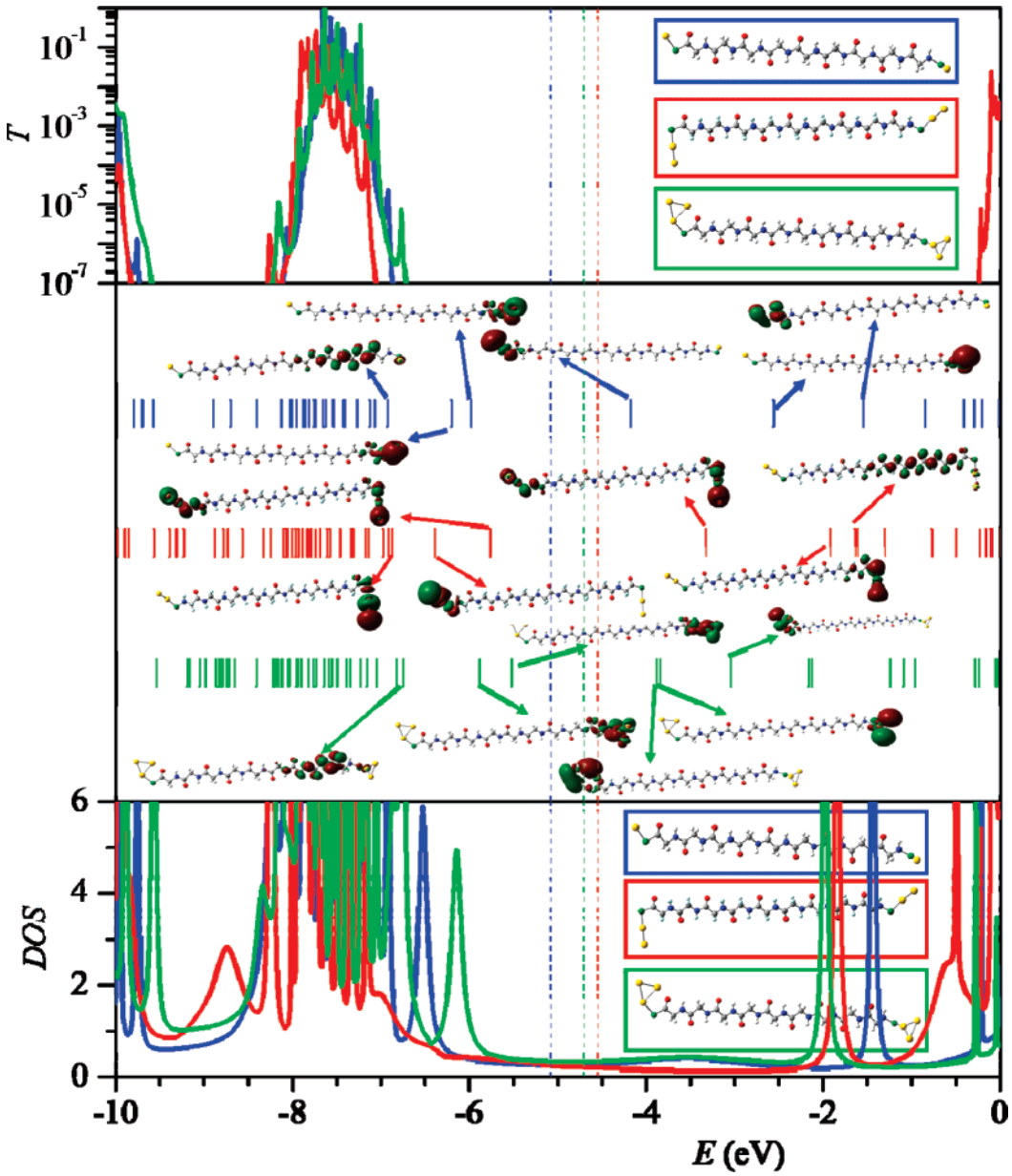

Figure 9. Electron transport characteristics of the $[Au_{bulk}Au_x]-[S-Gly_9-S]-[Au_xAu_{bulk}]$ molecular junctions: (top panel) electron transmission function; (middle panel) molecular orbitals and their corresponding orbital energies in the vicinity of the Fermi level; (bottom panel) DOS. The vertical dashed lines represent the Fermi level (taken as the middle point of the HOMO−LUMO gap of the extended molecules). The nature of electrodes is determined by the number of gold atoms directly contacting the molecule; curves are color coded: blue for $x = 1$, red for $x = 2$, and green for $x = 3$. All calculations are carried out at the B3PW91/LANL2DZ/6-31G* theory level of theory.

For the transmission function (Figure 3), a similar tendency is observed as the DOS. Below the Fermi energy, there are two sharp peaks for the molecular junction with $x = 3$; however, these two sharp peaks combined into a big flat peak for molecular junction with $x = 1$ and 2. And for the peaks above the Fermi level, we observe similar behavior as seen in its DOS; the positions of the peaks of the transmission functions are similar to those in the DOS.

What really differs is the magnitude of the transmission functions in the vicinity of the Fermi level. For molecular junction with $x = 1$ and 3, it shows similar values. However, for molecular junction with $x = 2$, it shows a big flat bunlike peak, therefore, contributing to the large value of current near 0 V.

The trimer shows quite different $I-V$ features from the monomer (Figure 4). For the trimer, only the molecular junctions with two direct contact gold atoms in the nanoelectrodes show ohmic behavior under low bias, and the other two cases yield Schottky barriers of about 2 V.

However, the molecules with two direct contact atoms have unpaired electrons on each of the nanoelectrodes. These unpaired electrons are loosely bonded and easy to transport through the molecule. For the other cases (with one and three contact atoms connected to the molecule), there are no unpaired electrons; thus, the electron transport probabilities are much lower than those with the unpaired electrons.

Furthermore, the trimer is about 10.8 Å in length, whereas the monomer is only 3 Å in length; thus, the probability for electrons to tunnel through the trimer will be much lower than tunneling through the monomer; the tunneling probability decays exponentially with the product of the length and the square root of the barrier height of the molecule.[39]

By comparing the frontier orbital energies and their corresponding orbital shape for the monomer and trimer (Figures 3

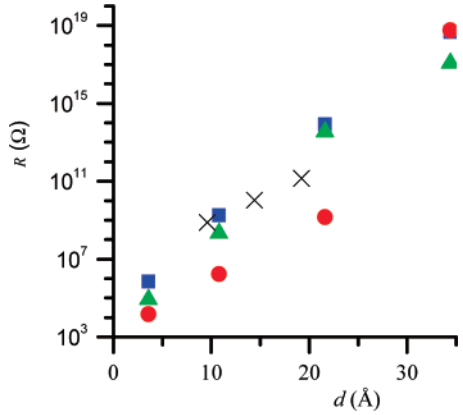

Figure 10. Molecular junction resistances vs length (from S to S ends) of dithioglycines $[Au_{bulk}Au_x]-[S-Gly_n-S]-[Au_xAu_{bulk}]$ ($n = 1, 3, 6,$ and 9, and $x = 1, 2, 3$) from this work and dithioalkanes $[Au_{bulk}Au_x]-[S-(CH_2)_n-S]-[Au_xAu_{bulk}]$ ($n = 8, 12, 16$ and $x = 1$) (ref 21) calculated at 1 V bias. (■) glycines with $x = 1$, (●) glycines with $x = 2$, (▲) glycines with $x = 3$, (×) for the alkanes with $x = 1$.

and 5), we find that both of them have similar Fermi energy and barrier height; thus, their differences in tunneling probability are mainly dependent on the length of the molecules.

For the short monomer, the tunneling probability is large, and ohmic $I-V$ behavior is observed. On the other hand, the probability for the trimer with one or two direct contact atoms on the nanoelectrodes is low; thus, Schottky $I-V$ characteristics are observed.

The trimer (Figure 5) also shows similar DOS and transmission functions as those of the monomer. Comparing Figures 3 and 5, we find out that both the DOS and the transmission function of the trimer are similar to those of the monomer.

Hexamer. For the hexamer, the observation that the molecular junctions with one or three gold atoms attaching to the molecule ends stands. Both hexamers show similar orbital energies, DOS, and transmission function (Figure 7).

However, the molecule with two gold atoms from the contact shows an extremely narrow band gap (~0.2 eV), quite different from the cases where one or three atoms from contact are connected to the ends of the molecules. These differences could also be observed from their DOS and transmission functions. As a result, the conductance of the molecule with two gold atoms at its ends is much higher than the conductance of the molecules having one or three gold atoms at their ends (Figure 6).

Nonamer. For the nonamer, quite different features are observed for the molecule with two gold atoms attached from the contact. Actually, the three cases of the nonamer show similar features of Fermi energies, band gap, DOS, and transmission functions (Figure 9); thus, the $I-V$ features of these three cases are similar to each other.

Since the nonamer length is ~34 Å, the interaction between the electrons occupying each end is very weak. Thus, the effects of the unpaired electrons are weak, and the differences between these three cases are negligible.

Current−Voltage Characteristics. From these calculations, we also find that the conductance of the molecules is very sensitive to the length of the molecules. The current decreases from milliamperes for the glycine monomer (Figure 2), to microamperes for the trimer (Figure 4), to nanoamperes for the hexamer (Figure 6), and picoamperes for nonamer (Figure 8).

By plotting their corresponding resistances at 1 V versus the length of the molecule (Figure 10), it is clearly shown that the current decreases almost exponentially as the length of the molecule increases. The exponential decay[21,40] is the direct result of electron tunneling through a barrier and takes place for most of the linear oligomers except for the smallest ones.[21]

It is interesting that molecular junctions of the same molecule with nanoelectrodes composed of one or three gold atoms show similar $I-V$ characteristics independent of the length of the molecule between the electrodes. Short oligoglycine ($n = 1$) in the junction shows ohmic behavior, whereas longer ones ($n = 3$, 6, and 9) show Schottky barriers.[41] The oligoglycines, but without double bonds along the molecular chain, are similar to the alkanes; however, despite the double bonds on the side chain of the former, electrons in the oligoglycines have to overcome a tunneling barrier.

If we take the center of the HOMO−LUMO gap as the Fermi level, and the HOMO for n-type carriers or LUMO for p-type carriers as the barrier height, the barrier height varies from about 0.2 eV for the molecular junctions with $x = 2$ and $n = 1$, 3, and 6, to about 1.5 eV for $x = 1$, 2 and $n = 1$, 3, 6, 9.

The Schottky barriers occur in all glycines with barriers but not in the monomer. For the monomer, only ohmic behavior is found since the monomer molecule is too short and the tunneling probability is high enough to behave as an ohmic resistance.

We also compared the resistances of the glycine molecular junctions with that of thioalkanes.[21] From Figure 10, it could be seen that the resistance of the molecular junctions approximately follow an exponential behavior for the glycine and thioalkane junctions.

However, the resistances are largely dependent on the nanoelectrodes. Regardless of the characteristics of the molecule between the two nanoelectrodes, the molecular junctions with the same number of gold atoms in contact have similar resistance.

It should be noticed that, as the number of gold atoms in contacts increases from one to two, the resistance changes almost 4 orders of magnitude. The high sensitivity of $I-V$ characteristics to the local conformation of the junction could explain the low reproducibility of experiments and calculations, which have been taking place since the beginning of the molecular electronics programs. At the atomistic scale, it is difficult to reproduce the local conformation of a nanojunction, and thus, it is equally difficult to reproduce its $I-V$ characteristics. Furthermore, the local structure of a nanoelectrode would vary as the experiment progresses because of the electromigration of the neutral metallic atoms composing the nanoelectrodes.[24]

4. Conclusions

We conclude that the $I-V$ characteristics of single molecular junctions depend on two major factors: the characteristics of the molecules and the local conformation of the nanoelectrodes. For molecular junctions built from oligoglycines, an exponential decay with respect to the molecular length is observed. The other factor that affects the $I-V$ characteristics is the local conformation of the nanoelectrodes used to fabricate the molecular junctions, especially the number of atoms that directly connect to the molecule. We find similar $I-V$ features for molecular junctions with one or three atoms in the nanocontacts; however, the $I-V$ features are quite different for molecular junctions with two atoms in the nanocontacts. We can also suggest based on the studied cases that nanoelectrodes with an unpaired number of electrons attaching to the molecule have higher conductance than those without paired number of electrons resembling doping in semiconductors. Having biological molecules as elements of electron transport provides the opportunity to fabricate electronic devices, sensors, and other

types of devices using already well-known and inexpensive fabrication techniques. In addition, the possibility to functionalize oligoglycines by attaching specialized molecular groups can strongly provide us the versatility needed for present needs of intelligent sensor devices.

Acknowledgment. We acknowledge financial support from the U.S. Army Research Office (ARO) and the U.S. Defense Threat Reduction Agency (DTRA).

References and Notes

(1) Reed, M. A.; Zhou, C.; Muller, C. J.; Burgin, T. P.; Tour, J. M. *Science* **1997**, *278*, 252.

(2) Mantooth, B. A.; Weiss, P. S. *Proc. IEEE* **2003**, *91*, 1785.

(3) Salomon, A.; Cahen, D.; Lindsay, S.; Tomfohr, J.; Engelkes, V. B.; Frisbie, C. D. *Adv. Mater.* **2003**, *15*, 1881.

(4) Selzer, Y.; Allara, D. L. *Annu. Rev. Phys. Chem.* **2006**, *57*, 593.

(5) Chen, F.; Hihath, J.; Huang, Z.; Li, X.; Tao, N. J. *Annu. Rev. Phys. Chem.* **2007**, *58*, 535.

(6) Tao, N. J. *Nat. Nanotechnol.* **2006**, *1*, 173.

(7) Seminario, J. M. *Nat. Mater.* **2005**, *4*, 111.

(8) Basch, H.; Ratner, M. A. *J. Chem. Phys.* **2003**, *119*, 11926.

(9) Seminario, J. M.; Cordova, L. E.; Derosa, P. A. *Proc. IEEE* **2003**, *91*, 1958.

(10) Husband, C. P.; Husband, S. M.; Daniels, J. S.; Tour, J. M. *IEEE Trans. Electron Devices* **2003**, *50*, 1865.

(11) Tour, J. M.; Van Zandt, W. L.; Husband, C. P.; Husband, S. M.; Wilson, L. S.; Franzon, P. D.; Nackashi, D. P. *IEEE Trans. Nanotechnol.* **2002**, *1*, 100.

(12) Seminario, J. M.; Yan, L.; Ma, Y. *IEEE Trans. Nanotechnol.* **2006**, *5*, 436.

(13) Seminario, J. M.; Yan, L.; Ma, Y. *Proc. IEEE* **2005**, *93*, 1753.

(14) Seminario, J. M. *Nat. Mater.* **2005**, *4*, 111.

(15) Chen, Y.; Jung, G.; Ohlberg, D. A. A.; Li, X.; Steward, D. R.; Jeppesen, J. O.; Nielson, K. A.; Stoddard, J. F.; Williams, A. R. *Nanotechnology* **2003**, *14*, 462.

(16) Kuekes, P. J.; Stewart, D. R.; Williams, R. S. *J. Appl. Phys.* **2005**, *97*, 034301.

(17) Derosa, P. A.; Seminario, J. M. *J. Phys. Chem. B* **2001**, *105*, 471.

(18) Seminario, J. M.; Derosa, P. A. *J. Am. Chem. Soc.* **2001**, *123*, 12418.

(19) Seminario, J. M.; Zacarias, A. G.; Derosa, P. A. *J. Chem. Phys.* **2002**, *116*, 1671.

(20) Seminario, J. M.; De La Cruz, C.; Derosa, P. A.; Yan, L. *J. Phys. Chem. B* **2004**, *108*, 17879.

(21) Seminario, J. M.; Yan, L. *Int. J. Quantum Chem.* **2005**, *102*, 711.

(22) Yan, L.; Seminario, J. M. *J. Phys. Chem. A* **2005**, *109*, 6628.

(23) Sotelo, J. C.; Yan, L.; Wang, M.; Seminario, J. M. *Phys. Rev. B* **2007**, *75*, 022511.

(24) Yan, L.; Seminario, J. M. *Int. J. Quantum Chem.* **2007**, *107*, 440.

(25) Seminario, J. M.; Araujo, R. A.; Yan, L. *J. Phys. Chem. B* **2004**, *108*, 6915.

(26) Shimizu, T.; Koqiso, M.; Masuda, M. Fibrous Microtube of Oligoglycine Compound. U.S. Patent 5876748, 1999.

(27) Yan, L.; Ma, Y.; Seminario, J. M. *J. Nanosci. Nanotechnol.* **2006**, *6*, 675.

(28) Seminario, J. M.; Yan, L.; Ma, Y. *J. Phys. Chem. A* **2005**, *109*, 9712.

(29) Seminario, J. M.; Tour, J. M. *Int. J. Quantum Chem.* **1997**, *65*, 749.

(30) Derosa, P. A.; Guda, S.; Seminario, J. M. *J. Am. Chem. Soc.* **2003**, *125*, 14240.

(31) Seminario, J. M.; Ma, Y.; Agapito, L. A.; Yan, L.; Araujo, R. A.; Bingi, S.; Vadlamani, N. S.; Chagarlamudi, K.; Sudarshan, T. S.; Myrick, M. L.; Colavita, P. E.; Franzon, P. D.; Nackashi, D. P.; Cheng, L.; Yao, Y.; Tour, J. M. *J. Nanosci. Nanotechnol.* **2004**, *4*, 907.

(32) Frisch, M. J.; Trucks, G. W.; Schlegel, H. B.; Scuseria, G. E.; Robb, M. A.; Cheeseman, J. R.; Montgomery, J. A., Jr.; Vreven, T.; Kudin, K. N.; Burant, J. C.; Millam, J. M.; Iyengar, S. S.; Tomasi, J.; Barone, V.; Mennucci, B.; Cossi, M.; Scalmani, G.; Rega, N.; Petersson, G. A.; Nakatsuji, H.; Hada, M.; Ehara, M.; Toyota, K.; Fukuda, R.; Hasegawa, J.; Ishida, M.; Nakajima, T.; Honda, Y.; Kitao, O.; Nakai, H.; Klene, M.; Li, X.; Knox, J. E.; Hratchian, H. P.; Cross, J. B.; Adamo, C.; Jaramillo, J.; Gomperts, R.; Stratmann, R. E.; Yazyev, O.; Austin, A. J.; Cammi, R.; Pomelli, C.; Ochterski, J. W.; Ayala, P. Y.; Morokuma, K.; Voth, G. A.; Salvador, P.; Dannenberg, J. J.; Zakrzewski, V. G.; Dapprich, S.; Daniels, A. D.; Strain, M. C.; Farkas, O.; Malick, D. K.; Rabuck, A. D.; Raghavachari, K.; Foresman, J. B.; Ortiz, J. V.; Cui, Q.; Baboul, A. G.; Clifford, S.; Cioslowski, J.; Stefanov, B. B.; Liu, G.; Liashenko, A.; Piskorz, P.; Komaromi, I.; Martin, R. L.; Fox, D. J.; Keith, T.; Al-Laham, M. A.; Peng, C. Y.; Nanayakkara, A.; Challacombe, M.; Gill, P. M. W.; Johnson, B.; Chen, W.; Wong, M. W.; Gonzalez, C.; Pople, J. A. *Gaussian-2003*, revision C.2; Gaussian, Inc.: Pittsburgh, PA, 2003.

(33) Becke, A. D. *J. Chem. Phys.* **1993**, *98*, 1372.

(34) Perdew, J. P.; Chevary, J. A.; Vosko, S. H.; Jackson, K. A.; Pederson, M. R.; Singh, D. J.; Fiolhais, C. *Phys. Rev. B* **1992**, *46*, 6671.

(35) Perdew, J. P.; Wang, Y. *Phys. Rev. B* **1992**, *45*, 13244.

(36) Legge, S. F.; Nyberg, G. L.; Peel, J. B. *J. Phys. Chem. A* **2001**, *105*, 7805.

(37) Francl, M. M.; Pietro, W. J.; Hehre, W. J.; Binkley, J. S.; Gordon, M. S.; DeFrees, D. J.; Pople, J. A. *J. Phys. Chem.* **1982**, *77*, 3654.

(38) Schlegel, H. B. *J. Comput. Chem.* **1982**, *3*, 214.

(39) Böhm, A. *Quantum Mechanics: Foundations and Applications*; Springer: New York, 1993.

(40) Wang, W.; Lee, T.; Reed, M. A. *Phys. Rev. B* **2003**, *68*, 35416.

(41) Sze, S. M. *Physics of Semiconductor Devices*, 2nd ed.; Wiley: New York, 1981.